Experimental Performance and Transient Analysis of Perched Cum Off-Center Wick Type Solar Still

C. Hariharan[1], B. Janarthanan[2] & C. Ramesh[3]

[1]Department of Physics, Jamal Mohamed College (Autonomous), Tiruchirappalli, India

[2]Department of Physics, Karpagam Academy of Higher Education, Coimbatore, India

[3]KIRND Institute of Research and Development, Tiruchirappalli, India

***DOI**: https://doi.org/10.34293/acsjse.v4i1.105*

Received Date: 07.01.2024 **Accepted Date:** 15.03.2024 **Published Date:** 01.04.2024

Abstract - *An effort has been taken to devise, engineer and construct a new single slope tilted-wick solar still incorporated with perched wick in the water reservoir to decrease the heat capacity and increase the evaporating surface to produce higher distillate yield. An effective analytical model is developed in the context of energy balance equation to study the momentary behavior of the proposed still. The influence of saline water stream rate on the concert of the still has been studied for various flow rates viz., 0.0025, 0.0035 and 0.0045 kg/s. The still shows good performance with higher distillate output for the rate of flow of saline water 0.0025 kg/s. Theoretical results based on the thermal model are intact with the experimental results and the model can be used to simulate the still in various locations, to optimize the design and operational parameters for long term installation.*

***Keywords**: Wick Type Solar Still, Saline Water Stream Rate, Distillate Yield.*

I INTRODUCTION

Solar energy is used for distillation of saline/brackish water. This is one of the most viable and economical technologies with least maintenance. Many solar stills with varying design parameters have been designed and fabricated by researchers and documented the results of the experimental and theoretical work to provide the best design for effective distillation of saline/brackish water. Based on the results of the documented work, still with wick materials in the basin has given promising output in the form of distillate yield by utilizing solar energy. Minasian and Al-Karaghouli (1995) have integrated the basin to hold the warm dissipated salt water from wick-type solar still. It is revealed that the wick basin solar has made pronounced yield related to the other solar still [1]. Mahdi et al. (2011) have studied the effect of mass flow rate of saline water and salinity on the productivity of the proposed still using charcoal cloth as evaporator in tilted-wick type solar still [2]. It has been reported that, increase in water stream rate and salinity decreases the efficiency and charcoal cloth is the best for absorber/evaporator in the still. A double slope basin type solar still with mild steel plate has been designed, constructed and weathered with light cotton sponge, coir, and waste cotton bits in the basin by KalidasaMurugavel and Srithar (2011). Results of the theoretical model based on the variation of transmittance of the condensing glass cover are found to be comparable with the experimental observations [3].

Manikandan et al. (2011) did a thorough review of wick-type solar stills which revealed the effectiveness and efficiency of wick-type solar stills more precisely [4].

Matrawyet al. (2015) have used corrugated evaporative surface using wick material and porous material to reduce the heat capacity [5]. It has been found that productivity increased by 34% compared to the ordinary basin type solar still. Zakaria Haddad et al. (2017) have used vertical rotating wick on the back wall of the still to get additional collector-evaporation area. The observations of the study inferred that the productivity improved by 14.72% in summer and 51.1% in winter compared to the still without vertical rotating wick [6]. Kaushalet al. (2017) have done experiments with wick basin with manifold effect heat recovery still and developed a correlation for productivity. Outcome of the study proved that the still has low payback period and an expense of about Rs. 4.25/kg for distillate yield [7]. They have also designed, fabricated and tested a modified floating wick vertical manifold effect diffusion solar still with waste water recovery and compared the performance with conventional design of basin type solar still. It has been found that the tailored design has produced distillate productivity of 21% greater than that of the conventional solar still [8].

Piyush Pal et al. (2018) designed a thermal model for the proposed double slope multi-wick solar still to examine the exergoeconomic and enviroeconomic behavior of the system. It has been concluded that the exergoeconomic parameter is 0.0623 and 0.0791 kWh/Rs for jute and cotton wicks in the still [9]. Piyush Pal et al. (2018) have done experiment on the double slope multi-wick basin solar still with black cotton and jute wick in the basin. Productivity of 4.5 l/m^2day of distillate yield were obtained for cotton wick and overall thermal efficiency was found to be 23.03% [10].

Qiushi Wang et al. (2018) have designed a new floating solar desalination film for large scale desalination for sea water demineralization and produced 1.38 kg/m^2day of distilled water production with comprehensive tracking of the sun [11]. Abdullah et al. (2019) have undergone vertical and horizontal rotation of jute cloth inside the solar distiller using a 6W DC powered by a photovoltaic system. Maximum efficiency of 82% is obtained under 30mm off time irrespective of the nanofluid in the still [12]. Abhay Agarwal and Rana (2019) have undergone experiment with multiple V-shaped floating wicks in single slope single basin solar still. Increased evaporating surface has produced higher distillate yield compared to the conventional solar still [13]. SivangiBishtet al. (2020) have found the effect of solar pond that influencing the production of distillate yield during night time of modified solar still with floating wicks in the basin. Results of the experiment revealed the increase in productivity of the still due to the contribution of solar pond for the supply of heat energy to the still all through night time [14]. KalpeshModiet al.(2020) have undergone experiments with two double basin single slope solar still with and without jute cloth [15]. Productivity of the still with pile of jute cloth increased by 8.89, 28.9 and 29.37% compared to still without jute cloth for three consecutive days in summer. Experiments were conducted with squared pyramid solar still using terry cotton, polyester,jute cloth and woolen as vertical wick materials in the basin with depth of 2cm by Saravanan and Murugan (2020). It has been found that woolen fabric in the basin produced higher distillate yield than other wick materials [16]. SwllamSharshir et al. (2020) have used aluminium, copper and steel metal chips pad in inclined wick solar still and studied the performance. Observations of the study revealed the maximum thermal efficiency of 60% for innovative wick-copper chips pad over

the conventional wick solar still [17]. Efforts have been taken to overcome the problems in the on hand solar stills to develop and fabricate a new perched cum off-center wick type solar still. In addition, energy balance equations have been written and solved for analytical solutions. Transient analysis has been attempted to find the thermal performance of the still.

II EXPLANATION OF THE DESIGN

A photograph of the experimental perched cum off-center wick is depicted in Figure 1. Single slope solar still with water reservoir has been constructed such that the tilted-wick has an inclination of 15° with respect to the horizontal. The water reservoir is filled with saline/brackish water and level is maintained just below the tilted portion to avoid the overflowing of water in the off-centered wick portion. Off center portion of the proposed still is covered with jute wick and perched wick is prepared as corrugated shape with thermocol sheet of thickness 2 cm and made to suspend on the surface of water in the reservoir. A valve has been fixed on the inlet of the water reservoir to maintain the required stream of briny water through the wick surface of the solar still. The perched wick surface also serves as the evaporating surface and intact with the water level in the reservoir. Hence the effective evaporation surface area is higher than that of the ordinary conventional wick-type solar still. The level of water in the tank is permitted in such a way to avoid the dehydration of the wick during max out bright hours. Moreover, the waste hot water at the end of the tilted-wick portion is fed into the reservoir so that the water can be treated preheated water for further distillation.

Figure 1 Photograph of the Perched Cum Off-Centered Wick Solar Still

III TRANSIENT THEORY

The wick surface is termed as the heart of the still and the wick absorbs the solar radiation communicated through the glass cover surface. Saline water through the wick surfaces by capillary action is heated up by utilizing heat energy absorbed. Water is evaporated and mass transfer takes place since it is condensed on the lower side of glass cover surface. The condensed water droplets trickle down in to the drainage channel and the distillate yield is collected using a measuring jar. To develop the thermal model, energy balance equations have been included with following assumptions

1. The evaporating wick surface and condensing glass are parallel to each other
2. There is no heat loss through the sides and bottom of the proposed solar still due to glass wool thermal insulation
3. Throughout the thickness of the condensing glass cover surface, the temperature is constant.
4. Mass transfer from evaporating surface is effectively taken place without any vapor leakage.

Temperature components of the proposed system have energy transfer and balance equation based on the energy transfer can be written as

Glass cover

$$\alpha_g I(t) b_g dx_3 + h_o (T_{ow} - T_g) b_o dx_1 + h_p (T_{pw} - T_g) b_p dx_2 = h_g (T_g - T_a) \quad (1)$$

Off-centered wick surface

$$\alpha_{ow} I(t) b_o dx_1 = m_{ow} C_w \left(\frac{dT_{ow}}{dx} \right) dx_1 + h_o (T_{ow} - T_g) b_o dx_1 + h_{bo} (T_{ow} - T_a) b_o dx_1 \quad (2)$$

Perched wick surface

$$\alpha_{pw} I(t) b_p dx_2 = m_{pw} C_w \left(\frac{dT_{wf}}{dx} \right) dx_2 + h_p (T_{pw} - T_g) b_p dx_2 + h_{bp} (T_{pw} - T_a) b_p dx \quad (3)$$

Where

$$h_o = h_{cow} + h_{eow} + h_{cow}$$

$$h_p = h_{cpw} + h_{epw} + h_{rpw}$$

$$h_{cow} = 0.884 \left[(T_{ow0} - T_g) + \frac{(P_{ow} - P_g)(T_{ow0} + 273)}{268900 - P_{ow0}} \right]^{1/3}$$

$$h_{cpw} = 0.884 \left[(T_{pw0} - T_g) + \frac{(P_{pw} - P_g)(T_{pw0} + 273)}{268900 - P_{pw}} \right]^{1/3}$$

$$h_{eow} = 0.016 \times h_{cow} \times \frac{P_{ow} - P_g}{T_{ow0} - T_g}$$

$$h_{epw} = 0.016 \times h_{cpw} \times \frac{P_{pw} - P_g}{T_{pw0} - T_g}$$

$$h_{row} = \frac{\varepsilon\sigma \left[(T_{ow0} + 273)^4 - (T_g + 273)^4 \right]}{(T_{ow0} - T_g)}$$

$$h_{rpw} = \frac{\varepsilon\sigma \left[(T_{pw0} + 273)^4 - (T_g + 273)^4 \right]}{(T_{pw0} - T_g)}$$

From Equation (1), we get

$$\overline{T_g} = \frac{\alpha_g I(t) b_g dx_3 + h_o T_{ow} b_o dx_1 + h_p T_{pw} b_p dx_2 + h_g T_a b_g dx_3}{h_o b_o dx_1 + h_p b_p dx_2 + h_g b_g dx_3} \quad (4)$$

The influence of Equation (4), Equations (2) and (3) can be modified as

$$U_{ow1}I(t)b_o + U_{ow2}T_a b_o = m_{ow}S_w\left(\frac{dT_{ow}}{dx}\right) + T_{pw}\left[\frac{-h_o h_p b_o b_p dx_2}{h_o b_o dx_1 + h_o b_p dx_2 + h_g b_g dx_3}\right] +$$

$$T_{ow}\left[h_o b_o - \frac{h_o^2 b_o^2 dx_1}{h_o b_o dx_1 + h_p b_p dx_2 + h_g b_g dx_3} + h_{bo} b_o\right] \quad (5)$$

and

$$U_{pw1}I(t)b_p + U_{pw2}T_a b_p = m_{pw}C_w\left(\frac{dT_{pw}}{dx}\right) + T_{ow}\left[\frac{-h_o h_p b_o b_p dx_1}{h_o b_o dx_1 + h_p b_p dx_2 + h_g b_g dx_3}\right] +$$

$$T_{pw}\left[h_p b_p - \frac{h_p^2 b_p^2 dx_2}{h_o b_o dx_1 + h_p b_p dx_2 + h_g b_g dx_3} + h_{bp} b_p\right] \quad (6)$$

Where

$$U_{ow1} = \alpha_{ow} + \frac{h_o \alpha_g b_g dx_3}{h_o b_o dx_1 + h_p b_p dx_2 + h_g b_g dx_3}$$

$$U_{ow2} = h_{bo} + \frac{h_o h_g b_g dx_3}{h_o b_o dx_1 + h_p b_p dx_2 + h_g b_g dx_3}$$

$$U_{pw1} = \alpha_{pw} + \frac{h_p \alpha_g b_g dx_3}{h_o b_o dx_1 + h_p b_p dx_2 + h_g b_g dx_3}$$

$$U_{pw2} = h_{bp} + \frac{h_p h_g b_g dx_3}{h_o b_o dx_1 + h_p b_p dx_2 + h_g b_g dx_3}$$

Equations (5) and (6) can be rearranged as follows

$$\frac{dT_{ow}}{dx} + A_1 T_{ow} + B_1 T_{pw} = X(t) \quad (7)$$

and

$$\frac{dT_{pw}}{dx} + A_2 T_{ow} + B_2 T_{pw} = Y(t) \quad (8)$$

Where

$$A_1 = \frac{\left\{h_o b_o - \frac{h_o^2 b_o^2 dx_1}{h_o b_o dx_1 + h_p b_p dx_2 + h_g b_g dx_3} + h_{bo} b_o\right\}}{m_{ow} C_w}$$

$$B_1 = \frac{\left\{\frac{-h_o h_p b_o b_p dx_2}{h_o b_o dx_1 + h_p b_p dx_2 + h_g b_g dx_3}\right\}}{m_{ow} C_w}$$

$$X(t) = \frac{U_{ow1}I(t)b_o + U_{ow2}T_a b_o}{m_{ow} C_w}$$

$$B_2 = \frac{\left\{ h_p b_p - \frac{h_p^2 b_p^2 dx_2}{h_o b_o dx_1 + h_p b_p dx_2 + h_g b_g dx_3} + h_{bp} b_p \right\}}{m_{pw} C_w}$$

$$A_2 = \frac{\left\{ \frac{-h_o h_p b_o b_p dx_1}{h_o b_o dx_1 + h_p b_p dx_2 + h_g b_g dx_3} \right\}}{m_{pw} C_w}$$

$$Y(t) = \frac{U_{pw1} I(t) b_p + U_{pw2} T_a b_p}{m_{pw} C_w}$$

β has been multiplied to Equation (8) and added to Equation (7) to get

$$\frac{d}{dx}(T_{ow} + \beta T_{pw}) + T_{ow}(A_1 + A_2\beta) + T_{pw}(B_1 + B_2\beta) = X(t) + \beta Y(t)$$

Assuming

$$A_1 + A_2\beta = D \tag{9}$$

$$B_1 + B_2\beta = D\beta \tag{10}$$

The equation led to the form as

$$\frac{d}{dx}(T_{ow} + \beta T_{pw}) + D(T_{ow} + \beta T_{pw}) = X(t) + \beta Y(t) \tag{11}$$

The analytical solution for Eq.11 is obtained as

$$(T_{ow} + \beta T_{pw}) = \frac{X(t) + \beta Y(t)}{D} + C\exp(-Dx) \tag{12}$$

At $x = 0, T_{ow} = T_{ow10}, T_{pw} = T_{pw0}$

We get

$$C = (T_{ow10} + \beta T_{pw0}) - \frac{X(t) + \beta Y(t)}{D} \tag{13}$$

Equation (12) is substituted with C to get,

$$(T_{ow} + \beta T_{pw}) = \frac{X(t) + \beta Y(t)}{D}\left[1 - \exp(-Dx)\right] + (T_{ow10} + \beta T_{pw0})\exp(-Dx) \tag{14}$$

β has two values and are

$$\beta_{\pm} = \frac{-(a_1 - b_2) \pm \sqrt{(a_1 - b_2)^2 + 4a_2 b_1}}{2a_2} \tag{15}$$

With two values of β, two values of D from Eq. (9) is obtained as

$$D_{\pm} = A_1 + \beta_{\pm} A_2 \tag{16}$$

Two values of β and D are reflected in Equation (14) to give

$$(T_{ow} + \beta_{+}T_{pw}) = \frac{X(t) + \beta_{+}Y(t)}{D_{+}}\left[1 - \exp(-D_{+}x)\right] + (T_{ow10} + \beta_{+}T_{pw0})\exp(-D_{+}x) \tag{17}$$

and

$$(T_{ow} + \beta\_T_{pw}) = \frac{X(t) + \beta\_Y(t)}{D\_}\left[1 - \exp(-D\_x)\right] + (T_{ow10} + \beta\_T_{pw0})\exp(-D\_x) \tag{18}$$

The solution for perched and off-center temperature is obtained by solving the Equations (17) and (18)

$$T_{ow} = \frac{-1}{(\beta_{+} - \beta\_)}\left\{\frac{X(t) + \beta_{+}Y(t)}{D_{+}}\left[1 - \exp(-D_{+}x)\right]\beta\_ + T_{ow10}\left[\beta\_\exp(-D_{+}x) - \beta_{+}\exp(-D\_x)\right] - \right.$$

$$\left.\frac{X(t) + \beta\_Y(t)}{D\_}\left[1 - \exp(-D\_x)\right]\beta_{+} + T_{pw0}\beta_{+}\beta\_\left[\exp(-D_{+}x) - \exp(-D\_x)\right]\right\} \tag{19}$$

and

$$T_{pw} = \frac{1}{(\beta_{+} - \beta\_)}\left\{\frac{X(t) + \beta_{+}Y(t)}{D_{+}} - \frac{X(t) + \beta_{+}Y(t)}{D_{+}}\exp(-D_{+}x) + \frac{X(t) + \beta\_Y(t)}{D\_}\exp(-D\_x) - T_{pw0}\beta\_\exp(-D\_x)\right.$$

$$\left. + T_{ow10}\exp(-D_{+}x) - T_{ow10}\exp(-D\_x) + T_{pw0}\beta_{+}\exp(-D_{+}x) - \frac{X(t) + \beta\_Y(t)}{D\_}\right\} \tag{20}$$

Average off-centered and perched-wick temperatures for the perched and off-centered wicks length L_1 and L_2 is calculated by

$$\bar{T}_{ow} = \frac{1}{L_1}\int_0^{L_1} T_{ow}\,dx \tag{21}$$

$$\bar{T}_{pw} = \frac{1}{L_2}\int_0^{L_2} T_{pw}\,dx \tag{22}$$

Integration and application of limits for the Equations (21) and (22), the average perched and off-centered wicks length L_1 and L_2 is obtained as

$$\bar{T}_{ow} = \frac{-1}{L_1(\beta_{+} - \beta\_)}\left\{\frac{L_1\beta\_\left[X(t) + \beta_{+}Y(t)\right]}{D_{+}} + \beta\_\left[\frac{X(t) + \beta_{+}Y(t)}{D_{+}^2}\left[\exp(-D_{+}L\ ) - 1\right]\right] + \frac{T_{ow10}\beta\_}{D_{+}}\left[1 - \exp(-D_{+}L_1)\right] + \frac{\beta_{+}\left[X(t) + \beta\_Y(t)\right]}{D\_^2}\left[1 - \exp(-D\_L_1\right] + \right.$$

$$\left.\frac{T_{ow10}\beta_{+}}{D\_}\left[\exp(-D\_L_1) - 1\right] + \frac{T_{pw0}\beta_{+}\beta\_}{D_{+}}\left[1 - \exp(-D_{+}L_1)\right] + \frac{T_{pw0}\beta_{+}\beta\_}{D\_}\left[\exp(-D\_L_1) - 1\right] - \frac{L_1\beta_{+}\left[X(t) + \beta\_Y(t)\right]}{D\_}\right\} \tag{23}$$

and

$$\bar{T}_{pw} = \frac{1}{L_2(\beta_{+} - \beta\_)}\left\{\frac{L_2\left[X(t) + \beta_{+}Y(t)\right]}{D_{+}} + \left[\frac{X(t) + \beta_{+}Y(t)}{D_{+}^2}\left[\exp(-D_{+}L_2) - 1\right]\right] + \frac{T_{ow10}}{D_{+}}\left[1 - \exp(-D_{+}L_2)\right] + \frac{\left[X(t) + \beta\_Y(t)\right]}{D\_^2}\left[1 - \exp(-D\_L_2\right] + \right.$$

$$\left.\frac{T_{ow10}}{D\_}\left[\exp(-D\_L_2) - 1\right] + \frac{T_{pw0}\beta_{+}}{D_{+}}\left[1 - \exp(-D_{+}L_2)\right] + \frac{T_{pw0}\beta\_}{D\_}\left[\exp(-D\_L_2) - 1\right] - \frac{L_2\left[X(t) + \beta\_Y(t)\right]}{D\_}\right\} \tag{24}$$

The efficiency of the still at the particular instant by utilizing the Eqs. (23) and (24) can be derived as

$$\eta = \left(\frac{h_{eow}(\overline{T}_{ow} - \overline{T}_g)A_{ow} + h_{epw}(\overline{T}_{pw} - \overline{T}_g)A_{pw}}{I(t)} \right) \times 100 \qquad (25)$$

IV RESULTS AND DISCUSSIONS

Experiments have been carried out with the proposed still and observations for solar radiation and temperature have been recorded using pyranometer and thermometer. Among the experimental days, one day in winterduring the month of January have used for numerical calculations. The design parameters of the proposed still are as follows

$\alpha_g = 0.05 = \alpha_{ow} = \alpha_{pw} = 0.85$; $h_{b1o} = h_{bp} = 0.77 \text{w/m}^{2^\circ}C$; $b_o = b_p = b_g = 1.03m$

$h_g = 5.7 + 3.8V_w$; $V_w = 1.4\ m/s$; $\varepsilon = 0.9$

$\sigma = 5.669 \times 10^{-8}\ \text{w/m}^2k^4$; $C_w = 4190\,J/Kg$; $dx_1 = L_1 = 0.769m$; $dx_2 = L_2 = 0.265m$

Intensity of solar radiation and the ambient temperature of the typical day is plotted with respect to the working hours of the day and shown in the Figure 2. Measured total solar radiation in horizontal surface and tilted surface radiation for tilt angle of 15° has been denoted as curve I and II in the Figure 3 respectively.The off-center surface solar radiation has been calculated using the point of view made by the beam radiation perpendicular to the normal of the condensing glass cover (θ_T) and the high point angle of the sun (θ_z). In the secondary axis, temperature is plotted and mentioned as curve III.

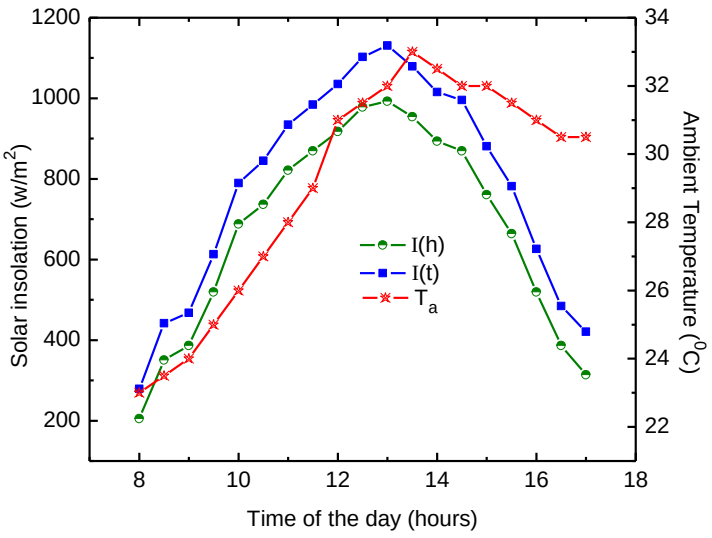

Figure 2 Variation of Climatic Parameter of the Operational Day of the Still

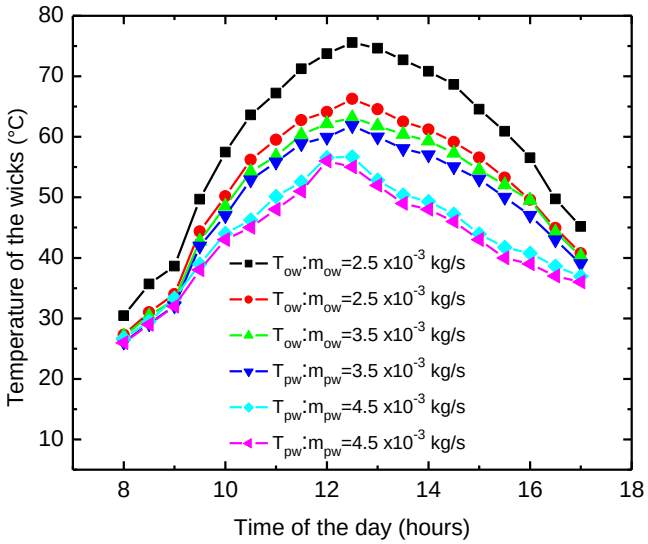

Figure 3 Variations of Temperature of the Wicks

Figure 4 shows the condensing glass cover temperature with respect to the operational hours of the day for the stream rate of 0.0025, 0.0035, 0.0045 kg/s. It has been seen that for lower stream rate of 0.0025 kg/s, temperature of the glass cover throughout the day is higher than that of the stream rates of 0.0035 and 0.0045 kg/s. This is due to the convective and radiative transfer of heat from the wick surfaces to condensing glass cover increases with decrease of stream rate by capillary action.

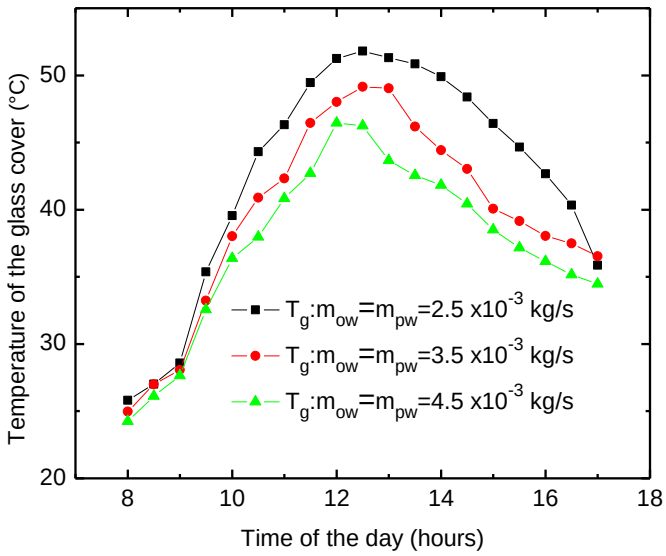

Figure 4 Condensing Surface Temperature for Different Stream of Saline Water

One of the inconveniences in conventional wick-type solar still i.e., scale formation of the salt beneath the wick surface and it is indispensable to remove the scaling of salt for every ten days to avoid the erosion of the base of the still. The proposed still is provided with corrugate shaped perched wick in the water reservoir and maximum salt deposited on the underside of the perched wick since the perched wick is made using the thermocol i.e., the

wick is stitched on the thermocol sheet of 2cm thickness. Due to the decreased salt deposition, scaling of salt over the off-centered wick portion is reduced more extensively. The variation of evaporative heat transfer coefficient with respect to the different stream rate of saline water is shown in the Figure 5. From the figure, it is confirmed that the evaporative heat transfer coefficient for least stream rate (0.0025kg/s) is pronounced compared to the other stream rates confirming the increase in evaporation with decrease of stream rate of saline water through the wick surface.

Convective and radiative coefficients have been determined and plotted with respect to operational hours of the day for the considered stream rates and depicted in Figure 6. It has been seen from the graph that, both convective and radiative coefficients has not shown any recurrence peaks throughout the day for different stream rates and thus confirmed the least significance to influence the temperature of the wick and condensing glass cover surface temperature. Among the three internal heat transfer coefficients, evaporative heat transfer coefficient is the effective parameter to influence the productivity of the proposed still and depends upon the heat capacity of the water in the still.

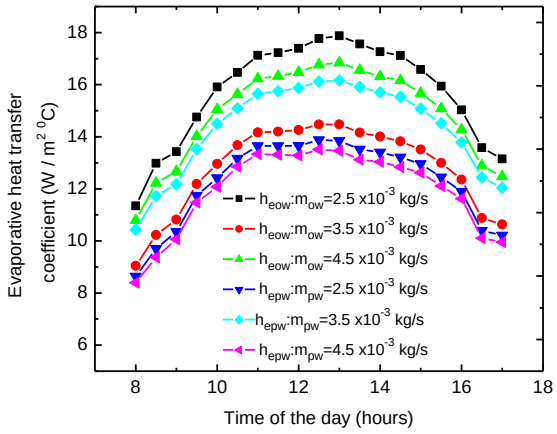

Figure 5 Effect of Mass Flow Rate on the Hourly Variation

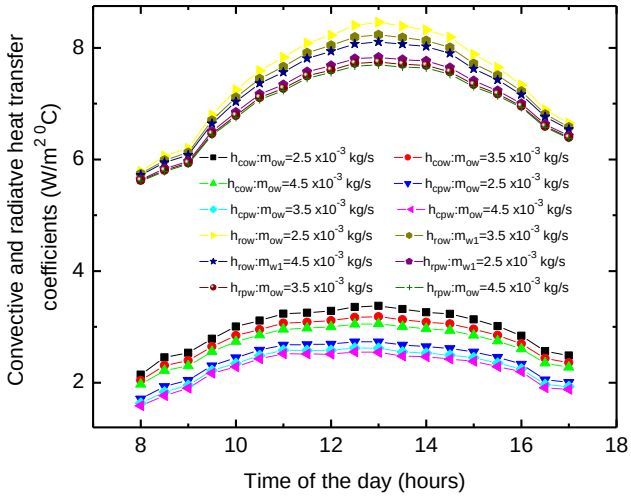

Figure 6 Effect of Mass Flow Rate on the Hourly Variations of Convective and Radiative Heat Transfer

Jute wick has been coated with mat black using the spray gun and homogeneous coating is obtained without affecting the capillarity of the wick. Transient model has been used to determine the productivity of the distillate yield with respect to that of the absorptivity of the wick surface. Absorptivity of the wick has been varied between the ranges from 0.35 to 0.85 with an interval of 0.10 and corresponding distillate yield has been found throughout the day.

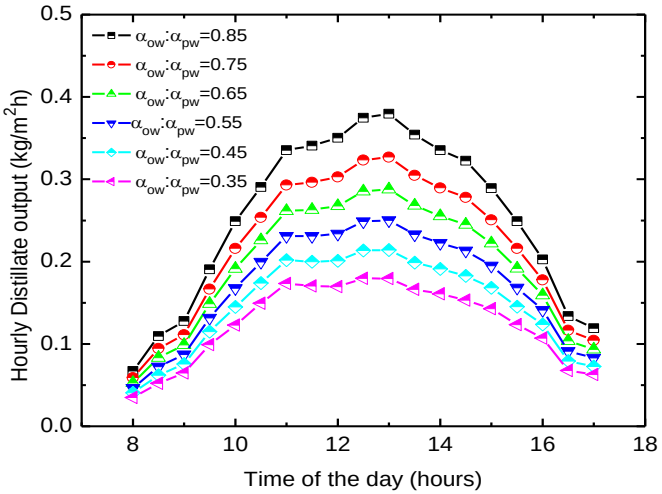

Figure 7 Effect of Absorptivity

Results of the distillate yield is plotted for the varying absorptivity of the wick with respect to that of the working hours of the day and depicted in Figure 7. From the Figure 7. it is clear that increase in absorptivity produces higher distillate yield with good thermal performance. Efficiency of the still at particular instant has been found for the respective stream rates considered and depicted in Figure 8. Efficiency for the stream rate of 0.0025 kg/S is found to be higher than that of the other increased stream rates and also higher throughout the day.

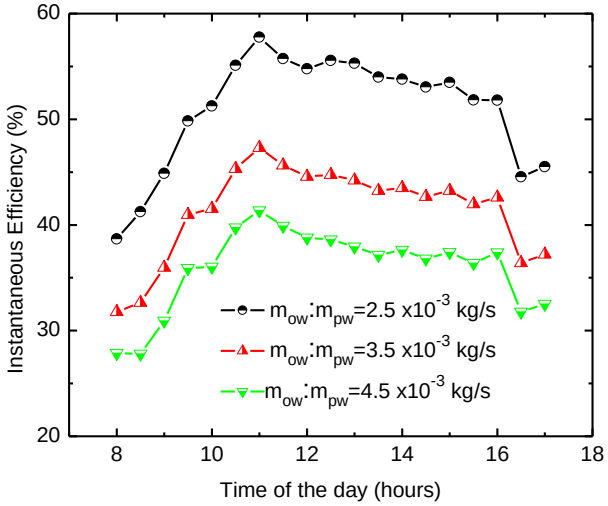

Figure 8 Effect of Mass Flow Rate on the Instantaneous Efficiency

V CONCLUSION

Experimental results and momentary behavior of the proposed still based on the developed theoretical model has given significant results and are

(i) Increase in effective evaporation area using perched wick in the water reservoir of the still served as an additional advantage to the proposed still.

(ii) The evaporative heat transfer has significant impact on the performance of the proposed still and mass transfer is taking place in this mode of heat transfer.

(iii) The effect of absorptivity of the evaporating wick surface has vital role to absorb solar radiation to a large extent.

(iv) From the results with respect to the stream rate, 0.0025 kg/s is optimum to produce higher distillate yield.

(v) The daily average efficiency of the still for 0.0025 kg/s is found as 50.95% which is higher than that of ordinary conventional wick type solar still.

Taken as a whole, thermal performance of the still is found to be good and the theory can be used to optimize the design and operational parameters of the proposed still for large scale installations.

VI REFERENCES

[1] Minasian, A. N., & Al-Karaghouli, A. A. (1995). An improved solar still: The wick-basin type. *Energy Conversion and Management*, *36*(3), 213-217.

[2] Mahdi, J. T., Smith, B. E., & Sharif, A. O. (2011). An experimental wick-type solar still system: Design and construction. *Desalination*, *267*(2-3), 233-238.

[3] Kalidasa Murugavel, K., & Srithar, K. (2011). Performance study on basin type double slope solar still with different wick materials and minimum mass of water. *Renewable Energy*, *36*(2), 612-620.

[4] Manikandan, V., Shanmugasundaram, K., Shanmugan, S., Janarthanan, B., & Chandrasekaran, J. (2013). Wick type solar stills: A review. *Renewable and Sustainable Energy Reviews, 20*, 322-335.

[5] Matrawy, K. K., Alosaimy, A. S., & Mahrous, A. F. (2015). Modeling and experimental study of a corrugated wick type solar still: Comparative study with a simple basin type. *Energy Conversion and Management, 105*, 1261-1268.

[6] Haddad, Z., Chaker, A., & Rahmani, A. (2017). Improving the basin type solar still performances using a vertical rotating wick. *Desalination, 418*, 71-78.

[7] Kaushal, A. K., Mittal, M. K., & Gangacharyulu, D. (2017). Productivity correlation and economic analysis of floating wick basin type vertical multiple effect diffusion solar still with waste heat recovery. *Desalination, 423*, 95-103.

[8] Kaushal, A. K., Mittal, M. K., & Gangacharyulu, D. (2017). An experimental study of floating wick basin type vertical multiple effect diffusion solar still with waste heat recovery. *Desalination, 414*, 35-45.

[9] Pal, P., Dev, R., Singh, D., & Ahsan, A. (2018). Energy matrices, exergoeconomic and enviroeconomic analysis of modified multi–wick basin type double slope solar still. *Desalination*, *447*, 55-73.

[10] Pal, P., Yadav, P., Dev, R., & Singh, D. (2017). Performance analysis of modified basin type double slope multi-wick solar still. *Desalination, 422,* 68-82.

[11] Wang, Q., Zhu, Z., & Zheng, H. (2018). Investigation of a floating solar desalination film. *Desalination, 447,* 43-54.

[12] Abdullah, A. S., Alarjani, A., Abou Al-sood, M. M., Omara, Z. M., Kabeel, A. E., & Essa, F. A. (2019). Rotating-wick solar still with mended evaporation technics: Experimental approach. *Alexandria Engineering Journal,* 58(4), 1449-1459.

[13] Agrawal, A., & Rana, R. S. (2019). Theoretical and experimental performance evaluation of single-slope single-basin solar still with multiple V-shaped floating wicks. *Heliyon,* 5(4).

[14] Bisht, S., Dhindsa, G. S., & Sehgal, S. S. (2020). Augmentation of diurnal and nocturnal distillate of solar still having wicks in the basin and integrated with solar pond. *Materials Today: Proceedings, 33*(3), 1615-1619.

[15] Modi, K. V., & Modi, J. G. (2020). Influence of wick pile of jute cloth on distillate yield of double-basin single-slope solar still: Theoretical and experimental study. *Solar Energy, 205,* 512-530.

[16] Saravanan, A., & Murugan, M. (2020). Performance evaluation of square pyramid solar still with various vertical wick materials - An experimental approach. *Thermal Science and Engineering Progress, 19.*

[17] Sharshir, S. W., Peng, G., Elsheikh, A. H., Eltawil, M. A., Elkadeem, M. R., Dai, H., Zang, J., & Yang, N. (2020). Influence of basin metals and novel wick-metal chips pad on the thermal performance of solar desalination process. *Journal of Cleaner Production, 248.*

Nomenclature

A_{ow} : Area of the off-centered wick surface (m^2)

A_{pw} : Area of the perched wick surface (m^2)

b_o : Breadth of off-centered wick surface (m)

b_p : Breadth of the perched wick surface (m)

b_g : Breadth of the glass cover (m)

C_w : Specific heat of water (J/Kg K)

dx_1 : Elemental length of the off-centered wick along x(m)

dx_2 : Elemental length of the perched wick along x(m)

dx_3 : Length of the glass cover (m)

h_o : Total heat transfer coefficient from off-centered wick water surface to glass cover (W/m^2K)

h_p : Total heat transfer coefficient from perched wick water surface to glass cover (W/m^2K)

h_g : Heat transfer coefficient from glass surface to ambient through insulation (W/m^2K)

h_{bo} : Heat transfer coefficient from off-centered wick water surfaceto ambient through insulation (W/m^2K)